Petroleum and Coal

**Article** **Open Access**

# A Comparative Permeability Modelling Study of the Enyenra Turonian Reservoirs, Tano Basin- Ghana

*Alberta Acheampong Boakye[1], Christopher O. Adeigbe[2], Frederick Kofi Bempong[3], Mark Kwesi Prempeh[4]*

[1] Geoscience Department, Pan African University Institute of Life and Earth Sciences (Including Health and Agriculture) (PAULESI), University of Ibadan, Ibadan, Nigeria
[2] Department of Geology, University of Ibadan, Ibadan, Nigeria
[3]Department of Petroleum Geosciences and Engineering, School of Petroleum Studies, University of Mines and Technology, Tarkwa, Ghana
[4] Geology Department, Ghana National Petroleum Corporation (GNPC), Tema, Ghana

Received April 21, 2021; Accepted October 7, 2021

**Abstract**

This study aimed at writing a suitable permeability model from well logs, and also comparing to select the best empirical permeability model for the Enyenra field. Four (4) empirical permeability models (Tixier, Timur, Coates and Dumanoir, and Wylie and Rose), poro-perm transforms and statistical means of predicting permeability values were applied to eight (8) well log data sets to ascertain the best model for the field. Petrophysical interpretation and Multilinear Regression (MLR) analysis were carried out with the data provided. Results obtained showed that the transform realised from the MLR equation provided the most suitable model for the field that could reduce cost in reservoir characterization. Also, the porosity- permeability cross-plots transforms were suitable for the cored wells while the Timur model was selected as the best predictive method among the empirical models compared. Furthermore, the five (5) lithofacies predicted across all wells from the Self Organizing Maps (SOM) were sandstone (argillaceous), siltstone, mudstone and claystone. Generally, the Turonian reservoirs of the Enyenra Field had good reservoir quality while lithofacies recorded values of permeability ranges of 50-100 mD.

***Keywords***: *Multilinear regression; Permeability; Tano Basin; Turonian; Petrophysics.*

## 1. Introduction

Permeability determination is an essential parameter in the process of carrying out reservoir characterization studies reservoir development [1]. It is defined as the measure of the ability of a rock to permit the passage of fluids through its pores [2]. Permeability affects almost all phases of formation evaluation, reservoir characterization and production performance and, there are various ways of estimating it. The common practice of estimating permeability is the use of well logs, cores and drill stem testing. Critical factors that influence permeability of geologic formation includes; pore size and geometry, mineralogy, sedimentary diagenesis, rock structure etc. [3]. Well tests and cores are best used in obtaining accurate permeability values. Though using well log data to derive permeability values is associated with reduced economic cost but this exercise gives a clue on the expected permeability values [4].

Some mathematical and practical approaches have been established in an attempt to understand the complexity of permeability computation [5,7-8]. Generally, two categories of equations are available i.e., the empirical and the statistical equations. However, recent approach adopts the artificial neural networks model-free function estimators called the "virtual measurement [6]. All these established methods have contributed to the understanding of the factors controlling permeability. Also, it is an illusion to have a universal relation for permeability and other dependent variable [6].

In the Tano Basin of Ghana, studies have been carried out that is related to permeability values estimation using various approaches [7-8]. Most of the approaches used in such studies did not explore the comparative applicability of some established methods in reservoirs of the Tano Basin. This gap, thus necessitated the need to compare and determine the best method that is suitable to predict permeability values from well logs across the study area. This study compared four known empirical methods [9-12] in permeability values prediction to suggest the best method for the Enyenra Turonian reservoirs. Furthermore, a statistical equation was developed and used to predict permeability values across the Enyenra Turonian reservoirs.

## 2. Geologic setting

The geographical location of the Tano Basin is such that it is bounded to the west by the Ivory Coast Basin and to the east by the Salt Pond Basin [13]. The Basin evolved through a diverse phase of tectonically driven alteration over geologic time. The basin was initially a pull-apart but was later modified by wrenching in the Cretaceous Period. The Basin is characterized by stratified Cretaceous to Eocene marine sedimentary rocks [14]. The Tano Basin is one of the prolific basins in Ghana and has been noted for its commercial productivity since December 2010 [15]. Reasons attributed to the overall favorable medium to high porosity and relatively high permeability reservoirs of the basin [16]. The study area (Fig. 1) is located in the western portion of the Tano Basin, in the present-day upper shelf to mid slope bathymetry. The Turonian play has been appraised as one of the promising plays in the Tano Basin [17]. The study area, which is the Enyenra field intercepts the Turonian play. According to Unpublished report by the Ghana National Petroleum Corporation (GNPC), the Enyenra discovery is a narrow, sinuous, lower to mid slope turbidite channel complex of Turonian age (Upper Cretaceous). The channel complex consists of heterogeneous, amalgamated and stacked channel sands deposited within an aggradational channel-levee complex.

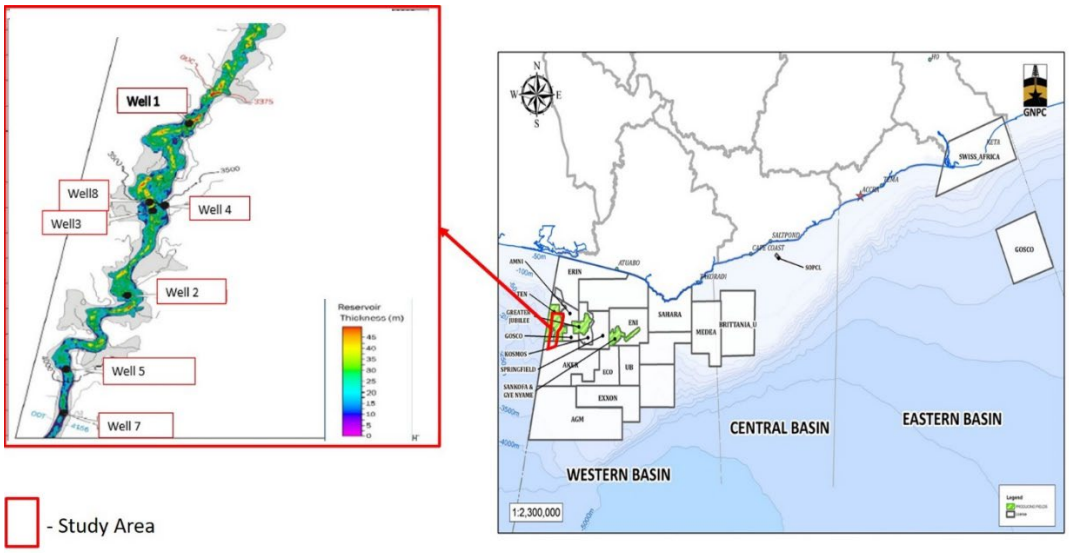


Fig. 1. Location map of study area showing the well location on the Enyenra Turonian reservoir (Source: GNPC, [17])

## 3. Data and methods

The study made use of eight (8) wells data with logs (Gamma Ray (GR), Neutron, Density, and Resistivity), software suite to facilitate interpretation and other necessary information provided by GNPC. Also, core data for four (4) wells were available to calibrate other Well data. In order to obtain a valid estimated permeability values, well logs were properly selected and calibrated with core data. While comparing core and log data, depth matching was critically done to avoid erroneous computations. Electro log templates were displayed to assist in

well log profile interpretation as shown in Fig. 2. The study was divided into two major folds: to use empirical models to compare and to generate a permeability equation statistically using well logs.

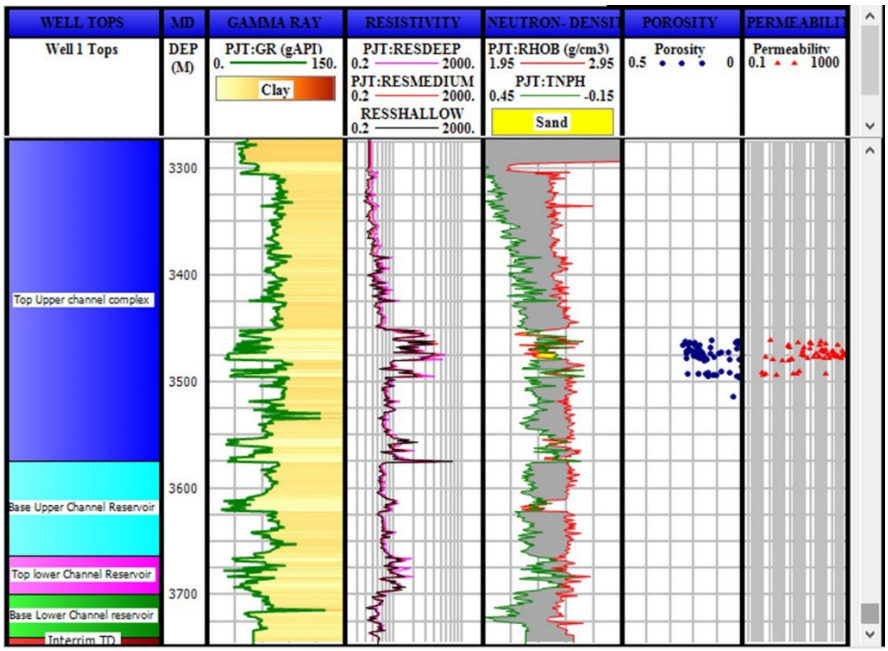


Fig. 2. A log template representation showing multiple logs acquired and some core porosity- permeability data for Well 1

### 3.1. Lithofacies identification and prediction using the Self Organizing Maps (SOM)

The rock types of the wells were analyzed and interpreted using neutron-density cross plot, RhoMatApp against DTMatApp cross plot and N/M cross plots. This was assisted by composite log and sedimentological data. To predict lithofacies calibrated to core, and to correlate rock types across the study area, the Self-Organizing Maps (SOM) unsupervised model was used to predict the lithofacies, which in turn inferred the permeability values in uncored intervals of the reservoirs. The GR, Density, Neutron were the main input log curves from each well. With SOM, each depth sample was identified with a particular node on the map within the study interval. The cluster randomness plot was then used to help select the ideal number of cluster groups to calibrate the SOM. This output dendrogram showed how the clustering of the SOM nodes has been performed [18].

### 3.2. Volume of clay/shale

The clay volume was calculated using the module "Clay volume analyses" from the IP™ software. Two different clay volumes were calculated with the module; one using values obtained from the GR log, and the other one using values obtained from the double clay indicators; density and neutron logs. The volume of shale further assisted to compute the porosity and water saturation. For the linear responses, Vshale is calculated using the GR as:

$$Vsh = \frac{GR_{\log} - GR_{min}}{GR_{max} - GR_{min}} \ldots \quad (i)$$

The Double Clay Indicators (DCI) is based on the principle of defining a clean line and a clay point. The clay volume is calculated as the distance where the input data falls between the clay point and the clean line.

$$VshND = \frac{(DenCl2 - DenCl1) * (Neu - NeuCl1) - (Den - DenCl1) * (NeuCl2 - NeuCl1)}{(DenCl2 - DenCl1) * (Neuclay - NeuCl1) - (Denclay - DenCl1) * (NeuCl2 - NeuCl1)}; \quad (ii)$$

where *DenCl*1 & *NeuCl*1 and *DenCl*2 & *NeuCl*2 are the density and neutron values for the two ends of the clean line.

### 3.3. Porosity

The porosity computation was done with density and neutron porosity logs, and it was calibrated with the overburden corrected core porosity.

Porosity $(ø) = (\frac{ø_N^2+ø_D^2}{2})\hat{}2$ … (iii)

### 3.4. Water saturation

The ratio of water volume by pore to water flow was calculated using the dual water saturation formula. The dual water approach was chosen because the Turonian reservoir is characterized by stacked shaly and sand formations. Two water resistivities were considered, the water occupied in the pore space and the water bounded to the shale.

Dual Water $= (\frac{1}{R_t} = ø_t^{mo} S_{wt}^{no}[\frac{1}{R_{wf}} + \frac{S_{wb}}{S_{wt}}\left(\frac{1}{R_{wb}} - \frac{1}{R_{wf}}\right)])$ (iv)

where øt = total porosity, Rt = formation resistivity, Swb = water bound saturation, mo = formation resistivity factor, no=saturation exponent, Rwb= apparent resistivity of water bound in clay

The density–neutron porosity was used as the porosity input. Rw was obtained iteratively by apparent method in wells with clear water leg coupled with Pickett plot (deep resistivity versus porosity).

$Rw=PHIT^2*Rt.$ (v)

### 3.5. Irreducible water saturation ($Sw_{irr}$)

Buckles' means of calculating irreducible water saturation from core data was adopted. The first task was to determine Buckles' constant from special core analysis in a clean pay zone. Therefore, KBUCKL (Buckles' constant) equaled the product of effective porosity (PHIE) and water saturation (Sw) from core data of each zone [19].

$Sw_{irr} = \frac{KBUCKL}{PHIE*(1-Vsh)}$… (vi)

### 3.6. Permeability, (K)

Permeability curves were computed for the four selected empirical formulae (i.e., Timur [11], Tixier [9], Wyllie & Rose [10] and Coates & Dumanoir [12]). Core permeability and porosity values were also used. The core permeability was adjusted to accommodate the overburden pressure at all wells. A plot of the corrected core permeability overburden versus corrected core porosity overburden was done. The regression line from the plot was analyzed to obtain using an exponential equation. The resultant equation line was then used to formulate a permeability log using the already measured total porosity as a key reference.

### 3.7. Multilinear regression method

Multilinear Regression module was used to predict the permeability resultant curve from a number of curves (GR, RHOB, PHIE, SW), using a least square regression routine. This routine estimated the best permeability curve which fits the input curves. After performing the multiple regression analyses, a supervised evaluation of the obtained permeability curve (equation) was performed using the determining coefficient ($R^2$). The $R^2$ which was 65 % makes the predicted regression equation helpful in predicting the Y (permeability) value.

### 3.8. Empirical models' comparative study

Empirical models encapsulate the relationship that exit among porosity, irreducible water saturation, and/or saturation exponent cementation factor in estimating formation permeability. The following highlights some established empirical relationships used.

#### 3.8.1. Timur's model

This model was developed by Timur [11]. Timur chose this equation based on the highest correlation coefficient and the lowest standard deviation. Thus, Timur [11] equation takes the form:

$$K = 8581 * \frac{\phi^{4.4}}{S_{wirr}^2}, \ldots \quad \text{(vii)}$$

where ϕ is porosity and $S_{wirr}$ is irreducible water saturation

### 3.8.2. Coates and Dumanoir model

Coates and Dumanoir, [12] proposed the permeability calculated as:

$$K^{0.5} = 100 \frac{\phi^2 (1 - S_{wirr})}{S_{wirr}} \ldots\ldots \quad \text{(viii)}$$

Concerning the irreducible water saturation of the formation used, this formula satisfies the assumption that zero porosity equals zero permeability when water saturation is 100%

### 3.8.3. Wyllie and Rose model

Wyllie and Rose [10] is a modification of the Kozeny- Carman model that considers the specific area's irreducible water saturation. The conventional means of direct calculation specific area is difficult to compute so the pore size was used instead. Pore size controls the irreducible water saturation [20].

$$\mathbf{K = (100} \frac{\phi^{2.25}}{(S_{wirr})} \mathbf{)^{2.}} \ldots \quad \text{(ix)}$$

### 3.8.4. Tixier model

Tixier [9] developed a simplified model upon the work of Wyllie and Rose [10], this equation was developed to create a continuous permeability log curve. The calculated permeability values from this Tixier equation is an average for the zone which corresponds to the resistivity gradient of the formation [6].

$$K^{0.5} = 250 \frac{\phi^3}{S_{wirr}} \ldots\ldots \quad \text{(x)}$$

## 4. Results and discussions

The results obtained and the interpretation made across the well that encountered the Turonian reservoir based on available data set used for this study will be discussed in this section.

### 4.1. Porosity estimation

The conformable overlap of the estimated porosity curve on the core porosity values confirms the validity of the estimated porosity from well logs (Fig. 3). This allow the porosity curve fit to be used in the estimation of the four empirical models in the study.

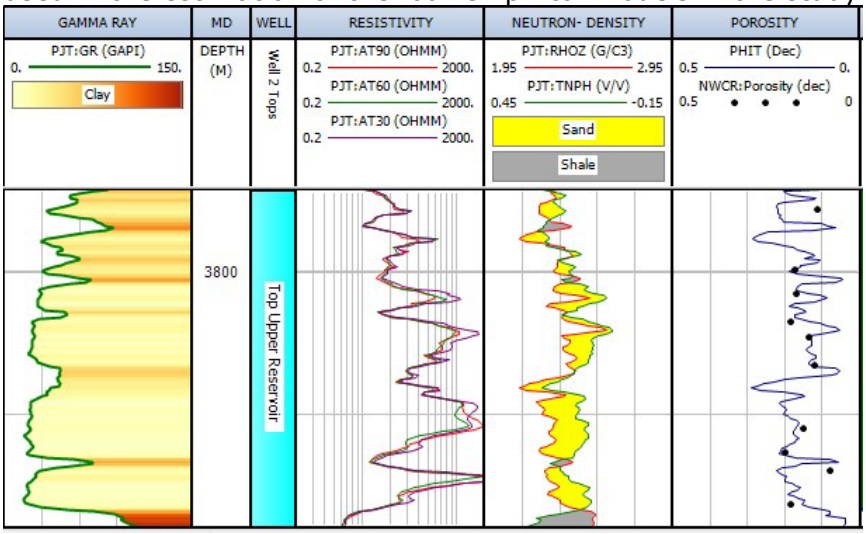


Fig. 3. Porosity curve overlain with corresponding dotted core porosity for Well 3

### 4.2. Core porosity – permeability cross plot

The permeability values were inferred and predicted from core porosity and permeability relationships. A relatively good trend was observed from the porosity (on a linear scale) against permeability (on a logarithmic scale) cross plot. The regression equation from each cored well used predicted a good continuous permeability curve as shown in Fig. 4.

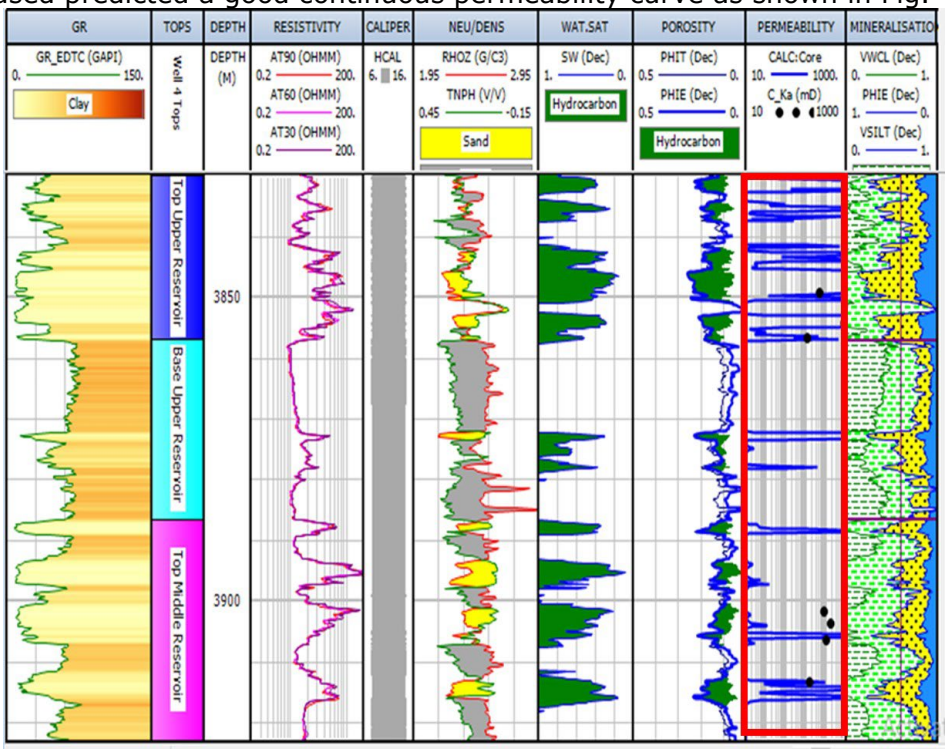


Fig. 4. The predicted permeability curve from core porosity and permeability cross plot for well 4 using the relation; 0.240858*EXP (38.75701*PHIT), where $R^2$= 0.8045

### 4.3. Comparison of empirical models in the various wells

Results obtained from the various wells after comparison suggested that, three out of the four empirical models were not suitable to predict permeability values for the Enyenra Turonian reservoirs. However, the Timur [11], is most suitable since it predicted permeability values closest to the core permeability values. Furthermore, permeability curves that were computed from porosity -permeability core correlation had a better match for the core results. Thus, it can be relied upon during permeability calculations for wells that are cored as shown in Table 2. The study also adopted the standard error means of comparing the empirical results. The larger the error margin, the less relevant the predicted value is to the actual data and vice versa. Table 2 gives the summary of the statistical calculations of standard error margin to core permeability- (empirical methods)

Table 1. Summary of permeability curves calibration with core.

| Well name | Permeability type | | | | |
|---|---|---|---|---|---|
| | Poro-Perm | Timur | Tixier | Coates&Dumanoir | Wyllie a Rose |
| Well 1 | | | | | |
| Well 2 | | | | | |
| Well 3 | | | | | |
| Well 4 | | | | | |

| Excellent | Very good | Good | Fair | Average |
|---|---|---|---|---|
| | | | | |

Table 2. Standard error margin to core permeability

| Standard error | Timur | Tixier | Coates&Dumanoir | Wyllie&Rose |
|---|---|---|---|---|
| MAD | 286.1082 | 317.2955 | 298.536662 | 333.0404438 |
| MSE | 290 055.9 | 295 434.9 | 301 112.18 | 302 450.2868 |
| RMSE | 538.5684 | 543.5393 | 548.736895 | 302 450.2868 |

where MAD is the mean average deviation; MSE is the mean squared error and RMSE is the root mean squared error

### 4.4. Multilinear regression analysis (MLR)

The Multilinear Regression analysis allowed the prediction of a resultant curve from a number of curves, using a least square regression routine. This routine estimated the best permeability curve which fits the input curves (Fig. 5). The MLR equation carved out is;

*10^ (11.80*Log (PHIT)+0.21*Log (SW)-21.72*Log (RHOB) - 0.38* Log (GR)) .* *(xi)*

where PHIT is total porosity; SW is water saturation; RHOB is density and GR is gamma ray.

The MLR equation predicted permeability curves that conform with the cored permeability values for the known cored four wells, thus this confirms the applicability to predict the permeability values across the Enyenra Turonian reservoir.

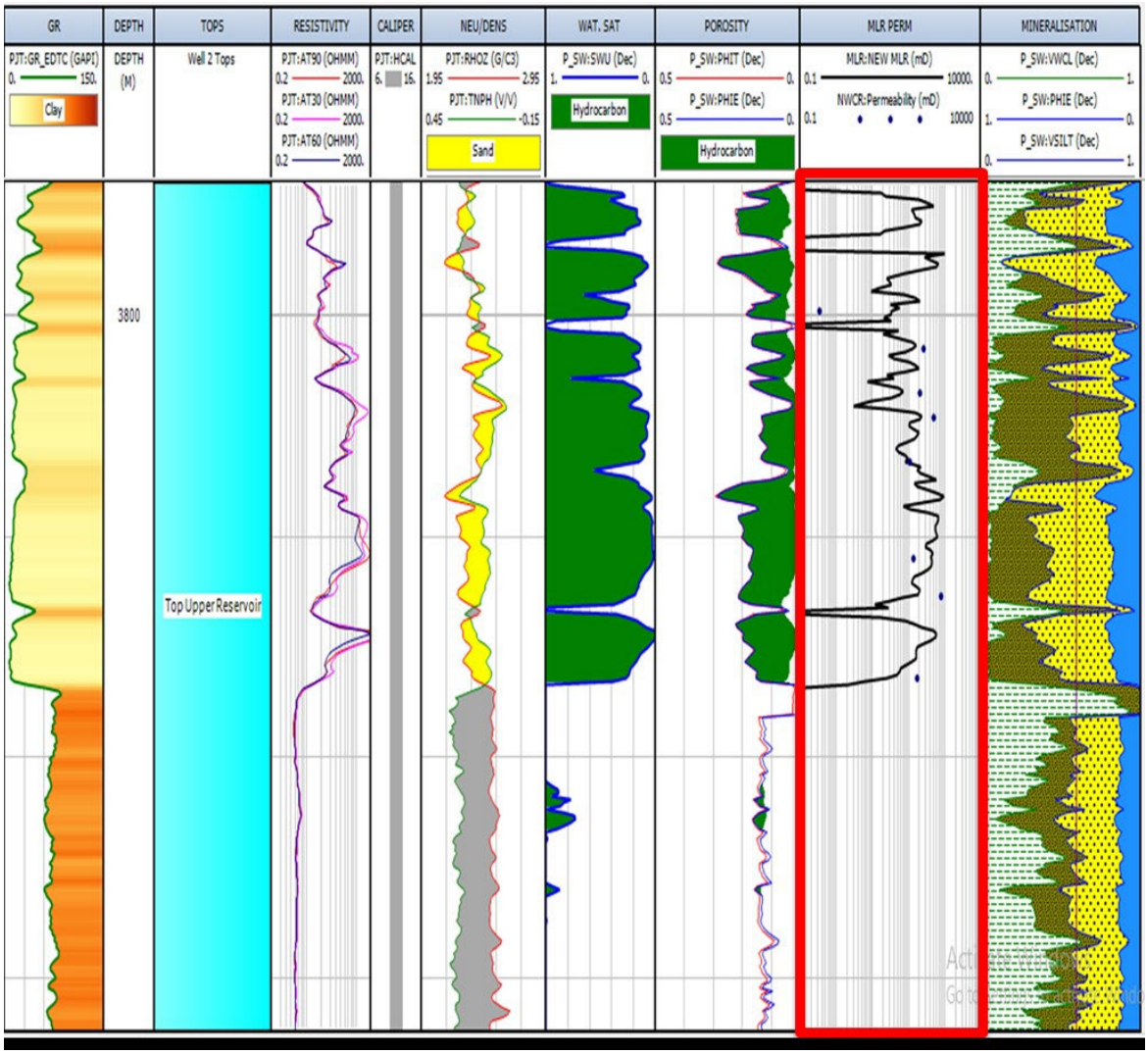


Fig. 5. Permeability curve estimated from the Multilinear Regression equation overlain with core permeability for Well 4

In this study, it can be seen from Table 3 that the density log is the most critical curve and thus contributed to most to the model generated. The closer the normalized coefficient is to 1, the more important that variable is and the closer the coefficient is to 0, the lower effective the variable is.

Table 3. Coefficients for the Multilinear regression analysis and their input variables with MLR Coefficient ($R^2$= 0.65)

| Input variable | Normalised coefficient |
|---|---|
| Constant | 0.3968 |
| Gama ray (GR) | 0.0040 |
| Bulk density (DENS) | 0.4206 |
| Neutron (NEUT) | 0.0125 |
| Total porosity | 0.0376 |
| Water saturation | 0.0282 |

### 4.5. Lithofacies prediction and description

The SOM method applied showed that the lithofacies inferred from the logs could be compared and linked to cored lithology. Five (5) lithofacies were predicted (Fig. 6 and 7). The facies predicted were grouped together at various depths and depositional environment. A comparison with core indicated that; lithofacies 1 and 2 predictions corresponded to sandstone and silty sandstone lithofacies respectively. These sandstones were deposited in a fairway – probably a submarine channel system, thus high permeability values were recorded for both core and predicted permeability curves. Lithofacies 3 predicted argillaceous sands while lithofacies 4 predicted interbedded mudstone and silty claystone, as lithofacies 5 was observed in some interval as claystone. Although Lithofacies 3 predicted sand package, the permeability values were low because the sands were intercalated with clay and mud, thus reducing the pore throat diameter, this is consistent with Dicus [21]. It is also important to note that lithofacies 4 and 5 had low permeability values which probably serve as seals for the Turonian reservoirs. The depositional environment in the study area is described as a submarine channel system with coarse sandy filling, which gradually declined into a more structured turbidite.

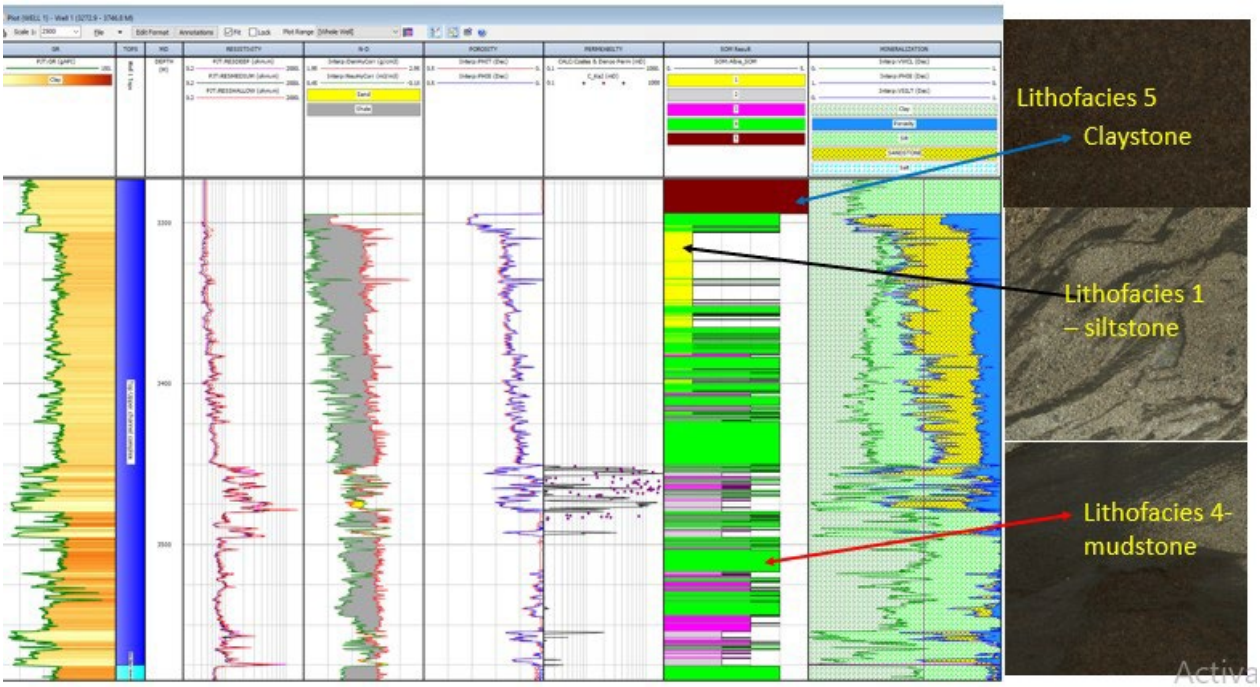


Fig. 6. SOM lithofacies correlated to core lithology. (Yellow colour siltstone, Green- mudstone and Brown-claystone) -Well 1

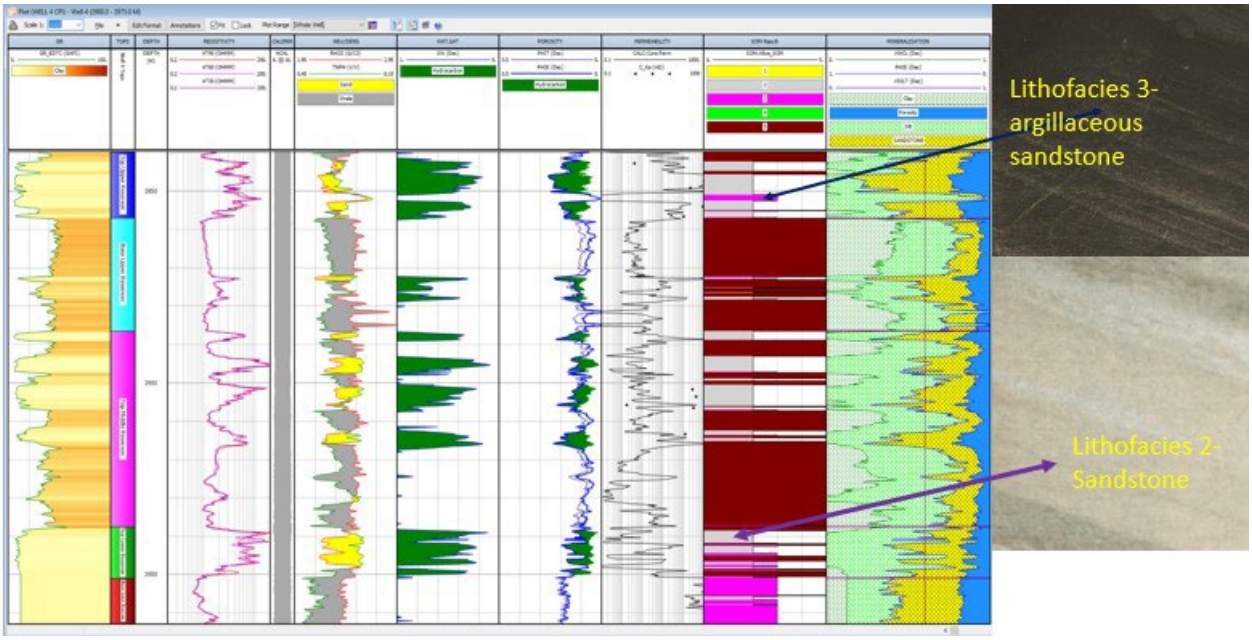


Fig. 7. SOM lithofacies correlated to core lithology (Fuchsia colour- argillaceous sandstone and Grey-sandstone)- Well 4

## 5. Conclusion

The predictive permeability model written and proposed for use across the Enyenra Turonian reservoirs, is the transform obtained from the Multilinear Regression equation. For Wells that are cored, the transform obtained from porosity- permeability cross-plots can be used to predict the permeability values. The Timur Model was selected as the best among the four empirical models to predict permeability in the study area due to its close predictive ability and low MSE percentage when compared to the core permeability data. The SOM predicted five (5) lithofacies. These lithofacies when compared to core samples showed that, lithofacies 1 and 2 corresponded to sandstone and silty sandstone respectively. Lithofacies 3 was argillaceous sandstone, lithofacies 4 was the interbedded mudstone (silty claystone) and lithofacies 5 was observed in an interval as claystone. The sedimentological and depositional characteristics of the predicted lithofacies conform to both core and calculated permeability values. However, the claystone, mudstone and the argillaceous sandstones had a relatively low permeability while the clean sandstones had high permeability. A further study to upscale this proposed permeability model and to test the practicability of the model in the neighbouring fields of the Tano Basin should be pursued.

***Acknowledgements***

*The first author expresses Her appreciation to the African Union Commission and the Pan African University, University of Ibadan, Nigeria for granting the opportunity and the funds used for the study. Also, we thank the Ghana National Petroleum Corporation for providing the data used, software utility, assisting and an enabling environment for the study to be accomplished.*

**Reference**


[1] Ghabezloo S, Sulem J, and Saint-Marc, J. Evaluation of a permeability-porosity relationship in a low-permeability creeping material using a single transient test. International Journal of Rock Mechanics and Mining Sciences, 2009; 46(4): 761–768.

[2] Alameedy, U. Permeability Evaluation of Zubair Formation Using Well Logs. European Association of Geoscientists and Engineers, 2012. Conference Proceedings, GEO 2012, Mar 2012, cp-287-00002.

[3] Ahmad, N. Permeability modeling of Lavrans field, Norway. An unpublished Masters' of Science Thesis submitted to the Faculty of Science and Technology, University of Stavanger, Norway, 2012

[4] Glover P. Permeability. Elsevier Geo-Engineering Book Series, 2006; 4: 231 -252

[5] Annan EB, Emmanuel A, and Ocran D. Mapping of Porosity, Permeability and Thickness Distribution: Application of Geostatistical Modeling for the Jubilee Oilfield in Ghana. Scientific and Academic Publishing, 2019; 9(2): 27–49

[6] Balan B, Mohaghegh S, and Ameri S. State-of-the-art in permeability determination from well log data: Part 1 - a comparative study, model development. Proceedings - SPE Eastern Regional Conference and Exhibition, 1995; 2(3): 33–42.

[7] Kuffour O. Estimation of Petrophysical Data for Assessing Hydrocarbon Potential in Western Ghana Oilfield (Tano Basin). An Unpublished Doctoral Dissertation submitted to the Graduate School of Kwame Nkrumah University of Science and technology (KNUST). 2008

[8] Anumah P, Mohammed S, Sarkodie KJ, Aggrey WN, and Morgan A. Petrophysical evaluation of the reservoir in the k - Field, offshore Ghana. Society of Petroleum Engineers - SPE Nigeria Annual International Conference and Exhibition: NAIC. 2019.

[9] Tixier MP. Evaluation of Permeability from Electric-Log Resistivity Gradients. Oil & Gas Journal, 1949; 16: 113.

[10] Wyllie MR, and Rose WD. Some theoretical considerations related to the quantitative evaluation of the physical characteristics of reservoir rock from electrical log data. Journal of Petroleum Technology, 1950; 2(04): 105-118.

[11] Timur A. An investigation of permeability, porosity, and residual water saturation relationships for sandstone reservoir. Well-Log Analysts, 1968; XXXX.

[12] Coats GR and Dumanoir JL. A New Approach to Improved Log-Derived Permeability: The Log Analyst, 1974, 15: 17 -31.

[13] Adda, GW. The Petroleum Geology and Prospectivity of the Neo-Proterozoic, Paleozoic and Cretaceous Sedimentary Basins in Ghana. Search and Discovery, 2013; 10544: 1–7.

[14] Kesse GO. The rock and mineral resources of Ghana, AA Balkema Publisher, Rotterdam, 1985. Netherlands, p. 610.

[15] Bempong FK, Ozumba BM, Hotor V, Takyi B, and Nwanjide CS. A Review of the Geology and the Petroleum potential of the Cretaceous Tano Basin of Ghana, J Pet Environ Biotechnol., 2019; 10: 1- 6.

[16] Tetteh JT. The Cretaceous Play of Tano Basin, Ghana. International Journal of Applied Sciences and Technology, 2016: 6 (1): 1-10.

[17] Ghana National Petroleum Cooperation (GNPC). The Lancet Neurology Reports 2013; 12(7): 634.

[18] Skalinski, Mark, Gottlib-Zeh, Stephanie, and Brian Moss. "Defining and Predicting Rock Types in Carbonates-an Integrated Approach using Core and Log Data in Tengiz Field." Paper presented at the SPWLA 46th Annual Logging Symposium, New Orleans, Louisiana, June 2005.

[19] Crain ER. The Log Analysis Hand Book Handbook; Penn- Well, Publ. Co., 1986, Tulsa

[20] Singh, NP. Permeability prediction from wireline logging and core data: a case study from Assam - Arakan basin. Journal of Petroleum Exploration and Production Technology, 2019; 9(1): 297–305.

[21] Dicus CM. Relationship Between Pore Geometry and Pore-Throat. AAPG Annual Convention, 2008; 40318: 27.


*To whom correspondence should be addressed: Miss Alberta Acheampong Boakye, Geoscience Department, Pan African University Institute of Life and Earth Sciences (Including Health and Agriculture) (PAULESI), University of Ibadan, Ibadan, Nigeria,* E-mail: albertaacheampong20@yahoo.com